THE JOURNAL OF BIOLOGICAL CHEMISTRY VOL. 286, NO. 52, pp. 45014–45029, December 30, 2011


# The Src Family Kinase Fyn Mediates Hyperosmolarity-induced Mrp2 and Bsep Retrieval from Canalicular Membrane*[S]

Received for publication, August 12, 2011, and in revised form, October 23, 2011 Published, JBC Papers in Press, November 4, 2011, DOI 10.1074/jbc.M111.292896

**Miriam Cantore**[1], **Roland Reinehr**[1], **Annika Sommerfeld, Martin Becker, and Dieter Häussinger**[2]

*From the Clinic for Gastroenterology, Hepatology, and Infectiology, Heinrich-Heine-University Düsseldorf, D-40225 Düsseldorf, Germany*

**Background:** Hyperosmotically induced hepatic cholestasis involves Mrp2 and Bsep retrieval from canalicular membrane.
**Results:** Hyperosmolarity induces NADPH oxidase isoform (NOX)-driven ROS-formation triggering Fyn-dependent bile acid transporter retrieval from canalicular membrane, which may be mediated by increased cortactin phosphorylation.
**Conclusion:** NOX, Fyn, and cortactin are critical players in hyperosmolarity-induced cholestasis.
**Significance:** New molecular insights in short term regulation of canalicular bile acid excretion are given.

**In perfused rat liver, hyperosmolarity induces Mrp2- (Kubitz, R., D'urso, D., Keppler, D., and Häussinger, D. (1997) *Gastroenterology* 113, 1438–1442) and Bsep retrieval (Schmitt, M., Kubitz, R., Lizun, S., Wettstein, M., and Häussinger, D. (2001) *Hepatology* 33, 509–518) from the canalicular membrane leading to cholestasis. The aim of this study was to elucidate the underlying signaling events. Hyperosmolarity-induced retrieval of Mrp2 and Bsep from the canalicular membrane in perfused rat liver was accompanied by an activating phosphorylation of the Src kinases Fyn and Yes but not of c-Src. Both hyperosmotic transporter retrieval and Src kinase activation were sensitive to apocynin (300 μmol/liter), *N*-acetylcysteine (NAC; 10 mmol/liter), and SU6656 (1 μmol/liter). Also PP-2 (250 nmol/liter), which inhibited hyperosmotic Fyn but not Yes activation, prevented hyperosmotic transporter retrieval from the canalicular membrane, suggesting that Fyn but not Yes mediates hyperosmotic Bsep and Mrp2 retrieval. Neither hyperosmotic Fyn activation nor Bsep/Mrp2 retrieval was observed in livers from p47$^{phox}$ knock-out mice. Hyperosmotic activation of JNKs was sensitive to apocynin and NAC but insensitive to SU6656 and PP-2, indicating that JNKs are not involved in transporter retrieval, as also evidenced by experiments using the JNK inhibitors L-JNKI-1 and SP6001255, respectively. Hyperosmotic transporter retrieval was accompanied by a NAC and Fyn knockdown-sensitive inhibition of biliary excretion of the glutathione conjugate of 1-chloro-2,4-dinitrobenzene in perfused rat liver and of cholyl-L-lysyl-fluorescein secretion into the pseudocanaliculi formed by hepatocyte couplets. Hyperosmolarity triggered an association between Fyn and cortactin and increased the amount of phosphorylated cortactin underneath the canalicular membrane. It is concluded that the hyperosmotic cholestasis is triggered by a NADPH oxidase-driven reactive oxygen species formation that mediates Fyn-dependent retrieval of the Mrp2 and Bsep from the canalicular membrane, which may involve an increased cortactin phosphorylation.**

Canalicular secretion in the liver is accomplished by the action of a variety of transport ATPases, such as the canalicular bile salt export pump (Bsep)[3] and the multidrug resistance protein 2 (Mrp2) gene-encoded organic anion export pump (for reviews, see Refs. 1–4). Expression of these pumps is regulated by lipopolysaccharide (5–7), dexamethasone (7, 8), drugs (9), and ambient osmolarity (10, 11). Short term regulation of canalicular bile acid excretion in perfused rat liver involves the effects of tauroursodeoxycholate (12) and liver cell hydration (13, 14). Hypoosmotic liver cell swelling increases within minutes the transport capacity for bile acids in a microtubule- and MAP kinase-dependent fashion, whereas hyperosmotic shrinkage is cholestatic (15, 16). These osmolarity effects on biliary secretion involve a rapid insertion/retrieval process of transporter molecules, such as Bsep and Mrp2 into/from the canalicular membrane (17, 18). Changes in liver cell hydration not only control biliary excretion but also hepatic metabolism, gene expression, and transport across the plasma membrane through activation of osmo-sensing and osmo-signaling pathways (for reviews, see Refs. 19, 20). Hypoosmotic liver cell swelling inhibits autophagic proteolysis and stimulates bile acid excretion and proliferation through integrin-dependent osmosignaling involving c-Src kinase, mitogen-activated protein (MAP) kinases (Erks, p38$^{MAPK}$), and the epidermal growth factor receptor (EGFR) (21, 22). On the other hand, hyperosmotic hepatocyte shrinkage leads to cholestasis (14, 17) and triggers plasma membrane translocation and activation of CD95, thereby sensitizing hepatocytes toward CD95 ligand (CD95L)-

* This work was supported by the Deutsche Forschungsgemeinschaft through Sonderforschungsbereich 575 "Experimentelle Hepatologie" and Klinische Forschergruppe 217 "Hepatobiliärer Transport und Lebererkrankungen" (Düsseldorf).

[S] The on-line version of this article (available at http://www.jbc.org) contains supplemental Figs. 1–4.

[1] Both authors contributed equally to this work.

[2] To whom correspondence should be addressed: Universitätsklinikum Düsseldorf; Klinik für Gastroenterologie, Hepatologie und Infektiologie; Moorenstrasse 5; D-40225 Düsseldorf, Germany. Tel.: 49-2118117569; Fax: 49-2118118838; E-mail: haeussin@uni-duesseldorf.de.

[3] The abbreviations used are: Bsep, bile salt export pump; Mrp2, rat canalicular isoform of the multidrug resistance protein; CD95, Fas (APO-1) receptor; CDNB, 1-chloro-2,4-dinitrobenzene; CDNB-GS, CDNB-glutathione conjugate; CLF, cholyl-L-lysyl-fluorescein; EGFR, EGF receptor; NAC, *N*-acetylcysteine; MAP, mitogen-activated protein; p38$^{MAPK}$, p38 MAPK; ROS, reactive oxygen species; ZO-1, polypeptide associated with the tight junction (zonula occludens); MAP, mitogen-activated protein; Ntcp, $Na^+$/taurocholate cotransport polypeptide.

induced apoptosis (23, 24). The molecular mechanisms underlying hyperosmotic CD95 activation have been studied in detail. Hyperosmolarity induces within seconds a chloride-driven acidification of early endosomes with subsequent activation of the acidic sphingomyelinase and formation of ceramide (25), which activates NADPH oxidase through a PKCζ-dependent phosphorylation of its activating subunit $p47^{phox}$ (25). NADPH oxidase-derived reactive oxygen species (ROS) trigger an activation of the Src family members Yes and Fyn and of the c-Jun-N-terminal kinase (JNK) (25, 26). Yes mediates transactivation of the EGFR, which associates with CD95 in a JNK-dependent manner (26). EGFR-driven CD95 tyrosine phosphorylation allows for CD95 oligomerization, translocation of the CD95/EGFR complex to the plasma membrane, where formation of the death inducing signaling complex (DISC) occurs (24). On the other hand, nothing is known about the signaling mechanisms, which mediate hyperosmotic Bsep and Mrp2 retrieval from the canalicular membrane and the role of Fyn, which becomes activated in response to hyperosmotic hepatocyte shrinkage. Fyn is, like the other Src kinase family members Src and Yes, ubiquitously expressed and these kinases share functional domains such as an N-terminal myristoylation sequence for membrane targeting, SH2 and SH3 domains, a kinase domain and a C-terminal noncatalytic domain (for reviews, see Refs. 27 and 28).

This study was undertaken to identify the molecular mechanisms underlying the hyperosmolarity-induced retrieval of the transporter molecules Bsep and Mrp2 from the canalicular membrane. Evidence is presented that mild hyperosmotic exposure results in a NADPH oxidase-driven and Fyn-mediated retrieval of both Bsep and Mrp2 from of the canalicular membrane, resulting in cholestasis.

## EXPERIMENTAL PROCEDURES

*Materials*—The materials used were purchased as follows: collagenases from Roche Applied Science; William's E medium and phalloidin-FITC from Sigma; penicillin/streptomycin from Biochrom (Berlin, Germany); fetal calf serum from Invitrogen; apocynin, SU6656, and PP-2 from Calbiochem; cholyl-L-lysyl-fluorescein (CLF) from BD Bioscience; L-JNKI-1 from Enzo Life Sciences (Lörrach, Germany), SP600125 from Tocris/Biozol (Eching, Germany), *N*-actetylcystein (NAC) and 1-chloro-2,4-dinitrobenzene (CDNB) from Sigma.

The antibodies used were purchased as follows: The Bsep/sister of P-glycoprotein (Spgp) (K12) polyclonal antibody was raised against an oligopeptide containing the C-terminal 13 amino acids coupled via cysteine to keyhole limpet hemocyanin and was a generous gift of Professor Dr. P. J. Meier and Dr. B. Stieger (University Hospital Zurich, Switzerland) (29). The EAG15 polyclonal antibody was raised against the 12-amino acid peptide sequence at the C terminus of the rat Mrp2 sequence as described previously (30) and was a generous donation from Prof. Dr. D. Keppler (Deutsches Krebsforschungszentrum, Heidelberg, Germany). Mouse anti-rat ZO-1 (31) was from Invitrogen. Cy3-conjugated AffiniPure goat anti-rabbit IgG (H + L) and FITC-conjugated goat anti-mouse IgG (H + L) were from Jackson ImmunoResearch Laboratories (West Grove, PA).

Antibodies recognizing phospho-$p38^{MAPK}$, phospho-JNK1/2, and total c-Src were from BioSource Int. (Camarillo, CA). The antibodies raised against total $p38^{MAPK}$, Yes (immunoprecipitation), and Fyn (immunoprecipitation) were from Santa Cruz Biotechnology (Santa Cruz, CA), against phospho-Src family-Tyr-418, phospho-Erk1/2, phospho-cortactin-Tyr-421, and total cortactin (immunoprecipitation) were from Cell Signaling (Beverly, MA), against total cortactin were from Millipore (Schwalbach, Germany), against total JNK1/2 were from BD Pharmingen, against total Erk1/2, Yes (Western blot), and Fyn (Western blot) were from Upstate Biotechnology (Lake Placid, NY), and against horseradish peroxidase-conjugated anti-mouse IgG and anti-rabbit IgG were from Bio-Rad. All other chemicals were from Merck at the highest quality available.

*Cell Preparation, Culture, and Transfection*—Hepatocytes were isolated from either the livers of male Wistar rats, wild type mice, or $p47^{phox}$ knock-out mice fed *ad libitum* with a standard diet by a collagenase perfusion technique as described previously (23). Aliquots of $1.5 \times 10^6$ cells were either plated on collagen-coated 6-well culture plates (Falcon, Heidelberg, Germany) and cultured for up to 24 h as published recently (primary rat hepatocytes (23)), or the amount of hepatocyte couplets was enlarged by decreasing the amount of collagenase to 0.05% according to Graf *et al.* (32), and cells were then plated on collagen-coated coverslips in 6-well culture plates (Falcon) or Matrigel (BD Biosciences)-coated MaTek dishes (MaTek Corp., Ashland, MA) and cultured for 6 h as published recently (32) before the experiments were started (primary rat hepatocyte couplets).

To knock down Fyn expression, hepatocyte couplets were transfected with either Fyn siRNA (#SI01514674) or negative control siRNA (#1027310) at final concentrations of 120 nmol/liter for up to 72 h using HiPerFect as transfection reagent according to supplier recommendation (Qiagen, Hilden, Germany).

Osmolarity changes were performed by appropriate addition or removal of NaCl from the medium. The viability of the hepatocytes was more than 95% as assessed by trypan blue exclusion.

*Rat and Mouse Liver Perfusion*—The experiments were approved by the responsible local authorities. Livers from male Wistar rats (120–150 g body mass) or wild type or $p47^{phox}$-knock-out mice fed a standard chow were perfused as described previously (33) in a non-recirculating manner. The perfusion medium was the bicarbonate-buffered Krebs-Henseleit saline plus L-lactate (2.1 mM) and pyruvate (0.3 mM) gassed with $O_2/CO_2$ (95/5 v/v). The temperature was 37 °C. In normoosmotic perfusions, the osmolarity was 305 mosmol/liter. Hyperosmotic exposure (385 mosmol/liter) was performed by raising the NaCl concentration in the perfusion medium. The addition of inhibitors to influent perfusate was made either by use of precision micropumps or by dissolution into the Krebs-Henseleit buffer. Viability of the perfused livers was assessed by measuring lactate dehydrogenase leakage into the perfusate, which did not exceed 20 milliunits $min^{-1}$ g $liver^{-1}$. The portal pressure was routinely monitored with a pressure transducer (Hugo Sachs Electronics, Hugstetten, Germany) (34). The effluent $K^+$ concentration and pH were continuously monitored

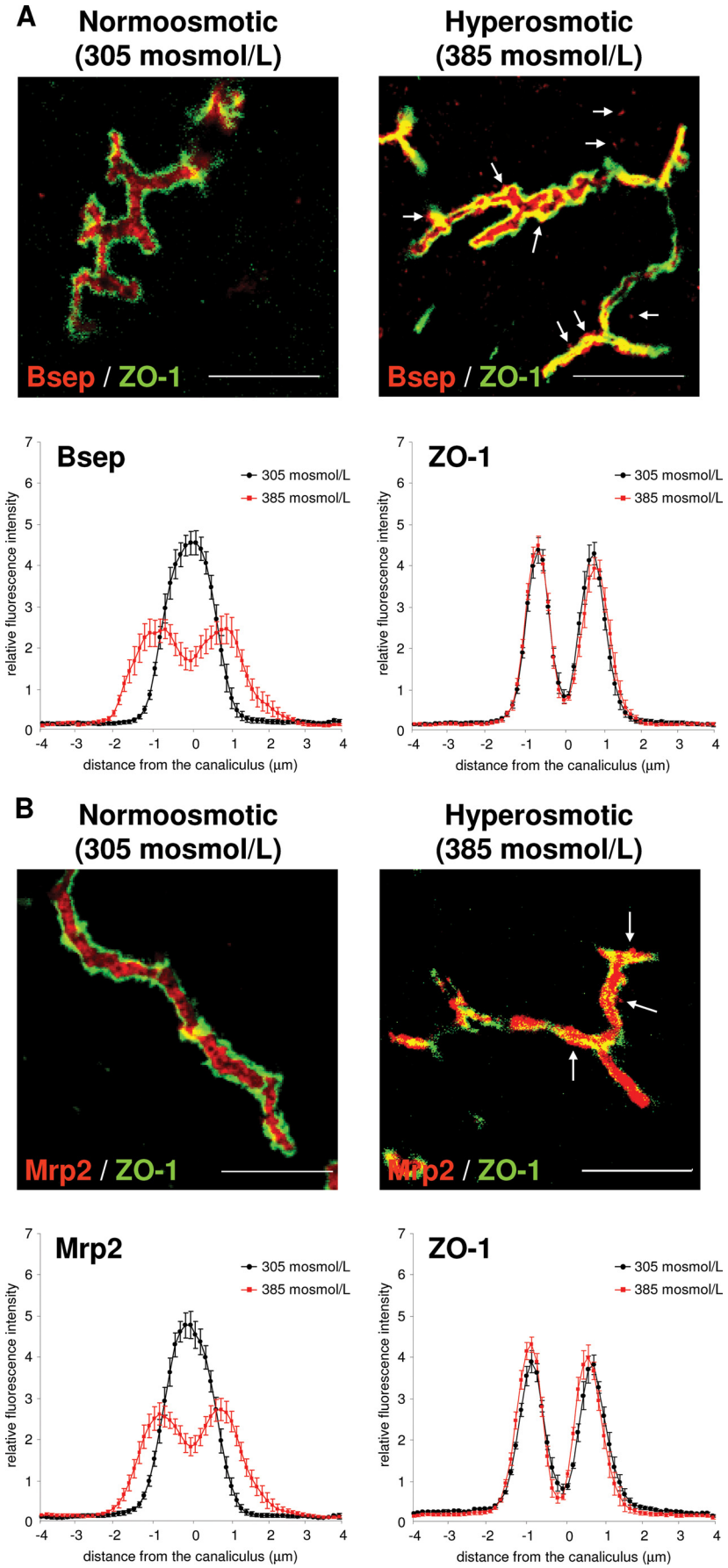
A
Normoosmotic
(305 mosmol/L)
Hyperosmotic
(385 mosmol/L)
Bsep / ZO-1
Bsep / ZO-1
Bsep
ZO-1
305 mosmol/L
385 mosmol/L
relative fluorescence intensity
distance from the canaliculus (μm)
B
Normoosmotic
(305 mosmol/L)
Hyperosmotic
(385 mosmol/L)
Mrp2 / ZO-1
Mrp2 / ZO-1
Mrp2
ZO-1

with respective electrodes (Radiometer, Munich, Germany). Ligation and excision of liver lobes was performed in a way that kept portal pressure constant, *i.e.* the perfusion flow was adjusted to maintain portal pressure constant.

In rat liver perfusion experiments with CDNB, bile ducts were cannulated, and samples were collected every 2 min from the bile and every minute from the effluent perfusate. CDNB (10 $\mu$mol/liter) was added to the influent perfusate using precision micropumps. The concentration of dinitrophenyl *S*-glutathione (GS-DNP, the glutathione conjugate of CDNB) was determined photometrically at 334 nm in bile and in the effluent as described previously (35, 36).

*Cryosectioning and Immunostaining of Rat Liver*—Tissue samples from perfused liver were cut at −20 °C in 7-$\mu$m sections using a Leica Cryotom CM 3050 (Leica, Bensheim, Germany) and placed on Superfrost plus slides (Menzel, Braunschweig, Germany). Slides were air-dried (1 h) and thereafter stored at −20 °C until staining. After fixation with pure methanol (−20 °C, 2 min), sections were washed with PBS and covered with fetal calf serum 5% in PBS for 30min. Sections were incubated for 2 h in a wet chamber with combinations of the primary antibodies, including anti-Bsep (K12, 1:200), anti-Mrp2 (EAG, 15 1:5000), and anti-ZO-1 (1:500). PBS alone or a single primary antibody was applied for control staining. After rinsing and washing, the slides were incubated for 1 h with a combination of Cy3-conjugated goat anti-rabbit IgG (1:500) plus FITC-conjugated goat anti-mouse IgG (1:100 each). After a final washing procedure, the sections were covered with mounting medium (1,4-diazabicyclo[2.2.2]octane (2%) in glycerol:PBS, 9:1) and a coverslip.

*Acquisition of Pictures*—Immunostained tissue sections were analyzed using the Zeiss LSM 510 META confocal laser scanning system. Images were acquired from 2 channels at 488- and 568-nm excitation wavelength. Emission was measured at 530 ± 10 nm (green) and >590 nm (red). Colocalization of the green (fluorescein) and red fluorescent dyes (Cy3) results in a yellow signal. Only samples that were prepared in parallel in all steps were compared using the same adjustments for all parameters (*i.e.* laser power, filter settings, setting of the acoustooptical tune-able filter, pinhole, lens, voltages at the photo multiplier tubes, number of accumulated scans, format size and zoom, scan speed, and z-step size when whole thickness of the tissue samples were analyzed). Pictures for densitometric analysis were prepared as follows; cryosections of rat livers were stained for the tight junction protein ZO-1, which forms the sealing border between canalicular and sinusoidal membrane. The areas to be analyzed were chosen by exciting the FITC molecules coupled to the anti-ZO-1 antibodies (via the secondary antibody). Apparent integrity and comparability of the canaliculi was assumed when the bordering tight junction lines (detected by the immunostained ZO-1) were intact, run in parallel, and showed a similar width that ranged from 1.26 to 2.01 $\mu$m (mean distance 1.52 ± 0.03 $\mu$m). No note was taken of the red immunostaining (Cy3) of Bsep or Mrp2. Images were coded to avoid bias during image selection. The person who recorded the microscopic images was unaware of the conditions of the experiments. Under continuous scanning, the upper and lower surfaces of the cryosections (distance ~7 $\mu$m) were determined using a remote-controlled, piezzo crystal-driven z-table mounted on the inverted microscope. The same area of the cryosection was then scanned at 15–20 consecutive levels that were 0.5 $\mu$m apart from each other. These pictures (containing red and green signals) were then calculated by use of the "projection" function of the Zeiss software to give a single picture, which was stored as TIF file. For each cryosection, condition data from 10 different sites were collected and used for further analysis.

*Densitometric Analysis of Confocal Pictures and Statistics*—Densitometry was performed as described previously (17, 18). For analysis of digitalized microscopic pictures of the canaliculi, the software Image-Pro Plus (Media Cybernetics, Baltimore, MD) was used. The profile of the fluorescence intensity was measured over a thick line at a right angle to the canaliculus. The length of the line was always 8 $\mu$m corresponding to 72 pixels with a pixel size of 0.11 $\mu$m (Bsep) or 8 $\mu$m corresponding to 130 pixels with a pixel size of 0.062 $\mu$m (ZO-1). To each of the pixels the mean fluorescence intensity over the line perpendicular to the length was calculated by Image-Pro Plus (separately for the green and red channel). The thickness of the line was adjusted to the individual canaliculus; only straight canalicular segments were chosen (straightness was normally given over 4–6 $\mu$m). The data obtained (pixel positions with the associated pixel intensities, red and green channel) were transferred to a MS-Excel data sheet. Each measurement was normalized to the sum of all intensities of the respective measurement. For the Bsep or Mrp2 fluorescence (red channel), the variances were calculated. The variances from different experimental conditions or from different time points of a perfusion experiment

FIGURE 1. **Immunohistochemical distribution of Bsep (*A*) and Mrp2 (*B*) in hyperosmotically perfused rat liver.** Rat livers were perfused for 30 min with either normo- (305 mosmol/liter; ○) or hyperosmolar Krebs-Henseleit buffer (385 mosmol/liter; ■) and immunostained for Bsep (*red*) and ZO-1 (*green*) (A) or for Mrp2 (*red*) and ZO-1 (*green*) (*B*), as given under "Experimental Procedures." Under normoosmotic conditions, Bsep (*A*) and Mrp2 (*B*) are largely localized between the linear ZO-1 staining/tight junction complex, whereas after hyperosmotic perfusion Bsep (*A*) and Mrp2 (*B*) appear aside the linear ZO-1 staining/tight junction complex (*arrow*) inside the cells. The pictures were obtained from single perfusion experiments. Experiments representative for a series of 12 individual experiments are shown. *White bar* = 10 $\mu$m. Densitometric analysis of fluorescence profiles and intensity of Bsep (*A*) and Mrp2 staining (*B*) is shown. Pictures were further analyzed densitometrically as described previously (17, 18). The *ordinate* shows normalized intensity of Bsep (*A*) or Mrp2-bound fluorescence (*B*) depending on the distance ($\mu$m) from the center of the canaliculus. Hyperosmotic perfusion (■, *red graph*) resulted in a significant lateralization of the Bsep (*A*)- or Mrp2-bound fluorescence (*B*). The fluorescence profiles depicted are statistically significantly ($p < 0.05$) different from each other with respect to variance and peak height. For control, livers were perfused for 30 min with normoosmotic medium (○, *black graph*). In these control experiments no significant change of Bsep (*A*) or Mrp2 fluorescence profiles (*B*) with respect of variance and peak height could be detected. Densitometric analysis of fluorescence profiles and intensity of ZO-1 staining (*A* and *B*) is shown. Distribution of ZO-1-bound fluorescence was analyzed at the canalicular area of longitudinally scanned canaliculi. The *ordinate* shows the normalized intensity of ZO-1 staining depending on the distance ($\mu$m) from the center of the canaliculus (set as 0). Under control conditions ZO-1 fluorescence profiles show two peaks, and liver perfusion experiments with either normo- (○, *black graph*) or hyperosmolarity (■, *red graph*) resulted in no significant changes of ZO-1 fluorescence profiles with respect to the distance of the peaks and to the variance of fluorescence profiles. Means of 40 measurements in each of the 12 individual experiments for each condition are shown (means ± S.E.). Statistical analysis was performed as described under "Experimental Procedures."

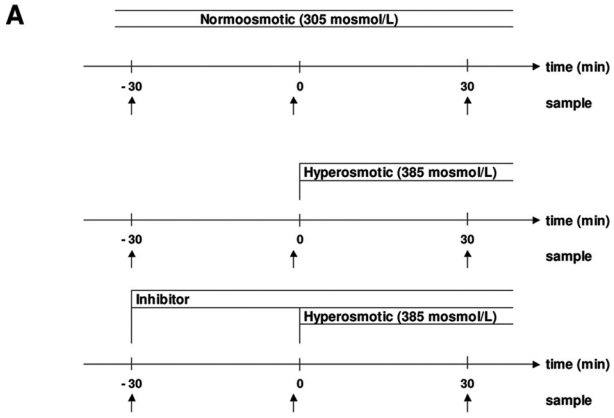
A
Normoosmotic (305 mosmol/L)
time (min)
-30
0
30
sample
Hyperosmotic (385 mosmol/L)
time (min)
-30
0
30
sample
Inhibitor
Hyperosmotic (385 mosmol/L)
time (min)
-30
0
30
sample

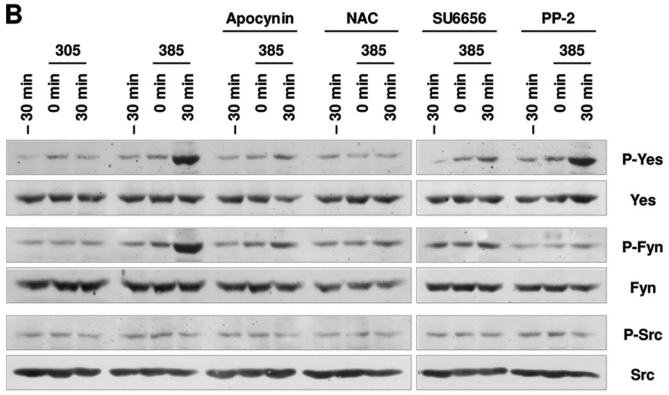
B
Apocynin
NAC
SU6656
PP-2
305
385
385
385
385
385
– 30 min
0 min
30 min
P-Yes
Yes
P-Fyn
Fyn
P-Src
Src

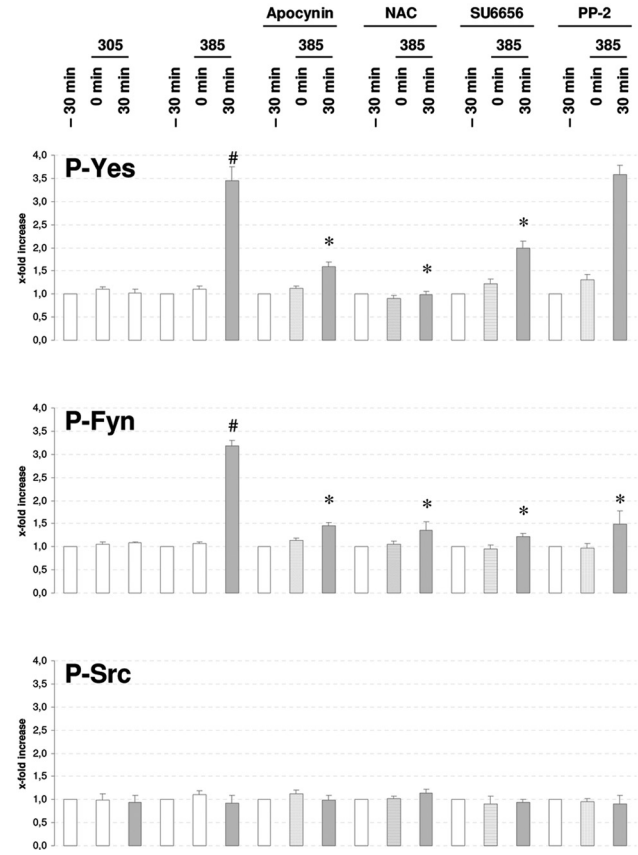
Apocynin
NAC
SU6656
PP-2
305
385
385
385
385
385
– 30 min
0 min
30 min
P-Yes
P-Fyn
P-Src
x-fold increase
4,0
3,5
3,0
2,5
2,0
1,5
1,0
0,5
0,0
#
*

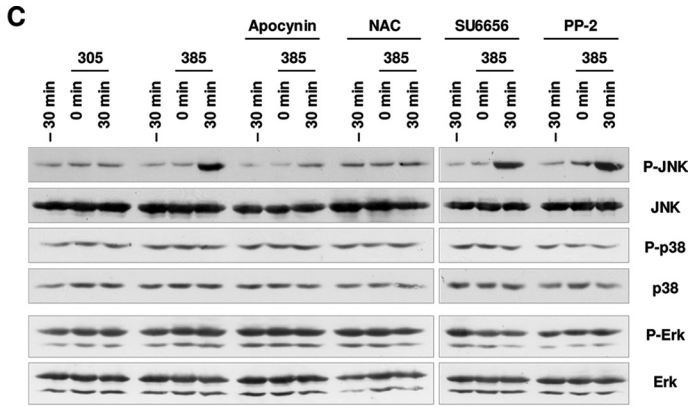
C
Apocynin
NAC
SU6656
PP-2
305
385
385
385
385
385
– 30 min
0 min
30 min
P-JNK
JNK
P-p38
p38
P-Erk
Erk

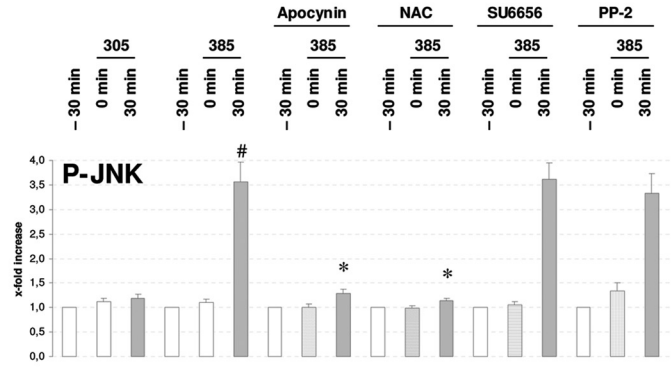
Apocynin
NAC
SU6656
PP-2
305
385
385
385
385
385
– 30 min
0 min
30 min
P-JNK
x-fold increase
4,0
3,5
3,0
2,5
2,0
1,5
1,0
0,5
0,0
#
*

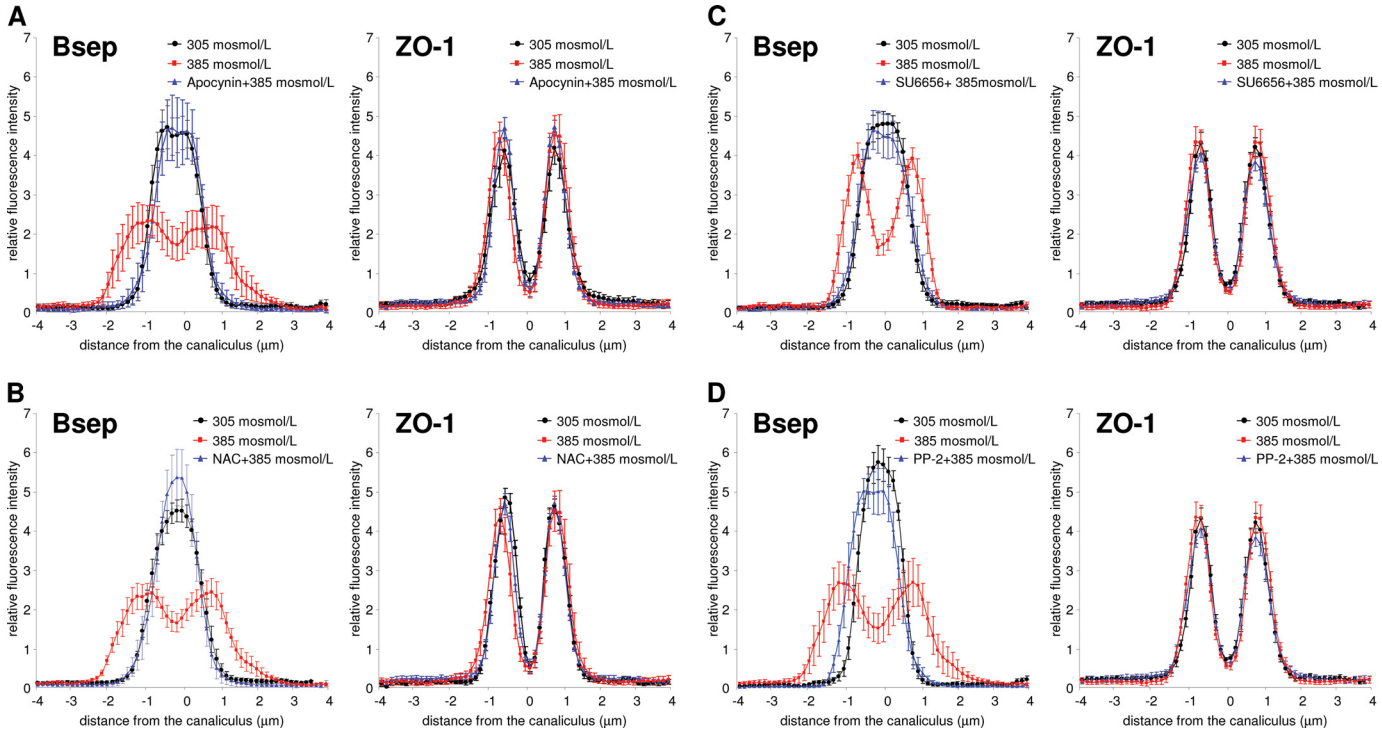


FIGURE 3. **Immunohistochemical determination of Bsep and ZO-1 distribution in hyperosmotic perfused rat livers.** Rat livers were perfused for 30 min with either normoosmotic medium alone (305 mosmol/liter; ○) or in the presence of an inhibitor (▲, *i.e.* apocynin (300 μmol/liter; *A*), NAC (10 mmol/liter; *B*), SU6656 (1 μmol/liter; *C*), or PP-2 (250 nmol/liter; *D*)). Thereafter, livers were perfused for another 30 min with either normo- (305 mosmol/liter; ○, *black symbols*) or hyperosmolar Krebs-Henseleit buffer (385 mosmol/liter) in the absence (■, *red symbols*) or presence of the respective inhibitors (▲, *blue symbols*). Bsep (*red*) and ZO-1 (*green*) were then immunostained and analyzed as given in Fig. 1. The means of 10 measurements in each of the 3 individual experiments for each condition (*A–D*) are shown (means ± S.E.). Apocynin (*A*), NAC (*B*), SU6656 (*C*), and PP-2 (*D*) all significantly inhibit hyperosmolarity-induced retrieval of Bsep from the canalicular membrane ($p < 0.05$), whereas these inhibitors by themselves did not significantly affect Bsep localization (see supplemental Fig. 3*A*) ($p > 0.05$). Ten measurements in each of three independent experiments for each condition were performed.

were compared by Wilcoxon's rank sum test. $p < 0.05$ was considered to be statistically significant. The canalicular diameters according to the distance of peak intensities of different experimental conditions or from different time points were compared by the two-sided Student's *t* test, whereas for the variance analysis of the profiles Wilcoxon's rank sum test was used. $p < 0.05$ was considered statistically significant. Data were obtained from at least three independent liver preparations.

*Western Blot Analysis*—Liver samples were transferred to sodium dodecyl sulfate (SDS)/polyacrylamide gel electrophoresis (PAGE), and proteins were blotted to nitrocellulose membranes using a semidry transfer apparatus (GE Healthcare) as recently described (23). Blots were blocked for 2 h in 5% (w/v) BSA containing 20 mmol/liter Tris, pH 7.5, 150 mmol/liter NaCl, and 0.1% Tween 20 (TBS-T) and then incubated at 4 °C overnight with the first antibody (antibodies used: anti-phospho-JNK1/2 and anti-phospho-Src family-Tyr-418 (1:1000), anti-Yes, anti-Fyn, anti-$p38^{MAPK}$ and anti-phospho-Src-Tyr-418 (1:2500), anti-phospho-Erk1/2 (1:5000)). After washing with TBS-T and incubation at room temperature for 2 h with horseradish peroxidase-coupled anti-mouse or anti-rabbit IgG antibody, respectively (all diluted 1:10,000), the blots were washed extensively and developed using enhanced chemiluminescent detection (GE Healthcare). Blots were exposed to Eastman Kodak Co. X-Omat AR-5 film.

*Immunoprecipitation*—Liver samples were harvested in lysis buffer containing 136 mM NaCl, 20 mM Tris-HCl, 10% (v/v) glycerol, 2 mM EDTA, 50 mM β-glycerophosphate, 20 mM sodium pyrophosphate, 0,2 mM Pefablock, 5 μg/ml aprotinin, 5 μg/ml leupeptin, 4 mM benzamidine, 1 mM sodium vanadate, and 1% (v/v) Triton X-100. The lysates were kept for 10 min on

FIGURE 2. **Hyperosmolarity-induced activation of Src and MAP kinases in the perfused rat liver.** Rat livers were perfused as described under "Experimental Procedures," and perfusion plans of the respective experiments are given in *A*. In detail, after 30 min of normoosmotic perfusion (305 mosmol/liter), a first liver tissue sample was taken (control, *t* −30 min). Then, livers were perfused for another 30 min under normoosmotic conditions in the absence or presence of the indicated inhibitors, and a second liver sample was taken (control, *t* 0 min or inhibitor, *t* 0 min). The inhibitors used were apocynin (300 μmol/liter), NAC (10 mmol/liter), SU6656 (1 μmol/liter), and PP-2 (250 nmol/liter). Thereafter, hyperosmolarity (385 mosmol/liter) was instituted for another 30 min, and a third liver tissue sample was removed (*t* 30 min). Liver samples were then analyzed for activation of Src kinase family members Yes, Fyn, and c-Src (*B*) and for activation of the MAP kinases JNK, $p38^{MAPK}$, and Erk (*C*). Blots were analyzed densitometrically. *t* −30 min, *i.e.* sample before institution of either hyperosmolarity or inhibitor, was set to 1. Representative blots and densitometric analysis of three independent perfusion experiments are shown. *B*, in line with previous studies (26), hyperosmolarity induced within 30 min a significant phosphorylation of Yes and Fyn (#, $p < 0.05$, $n = 3$), whereas no c-Src activation was observed ($p > 0.05$, $n = 3$). Phosphorylation of Yes and Fyn was sensitive to apocynin and NAC (*, $p > 0.05$, $n = 3$). Yes and Fyn phosphorylation was inhibited by SU6655 (*, $p < 0.05$, $n = 3$), whereas PP-2 inhibited hyperosmotic Fyn (*, $p < 0.05$, $n = 3$) but not Yes activation ($p > 0.05$, $n = 3$). *C*, in line with the literature (24), hyperosmotic exposure led within 30 min to a phosphorylation of JNK (#, $p < 0.05$, $n = 3$), whereas no $p38^{MAPK}$ or Erk phosphorylation occurred ($p > 0.05$, $n = 3$; densitometric analysis not shown). This JNK activation was sensitive to apocynin and NAC (*, $p < 0.05$, $n = 3$). SU6656 and PP-2 had no effect on JNK phosphorylation ($p > 0.05$, $n = 3$).

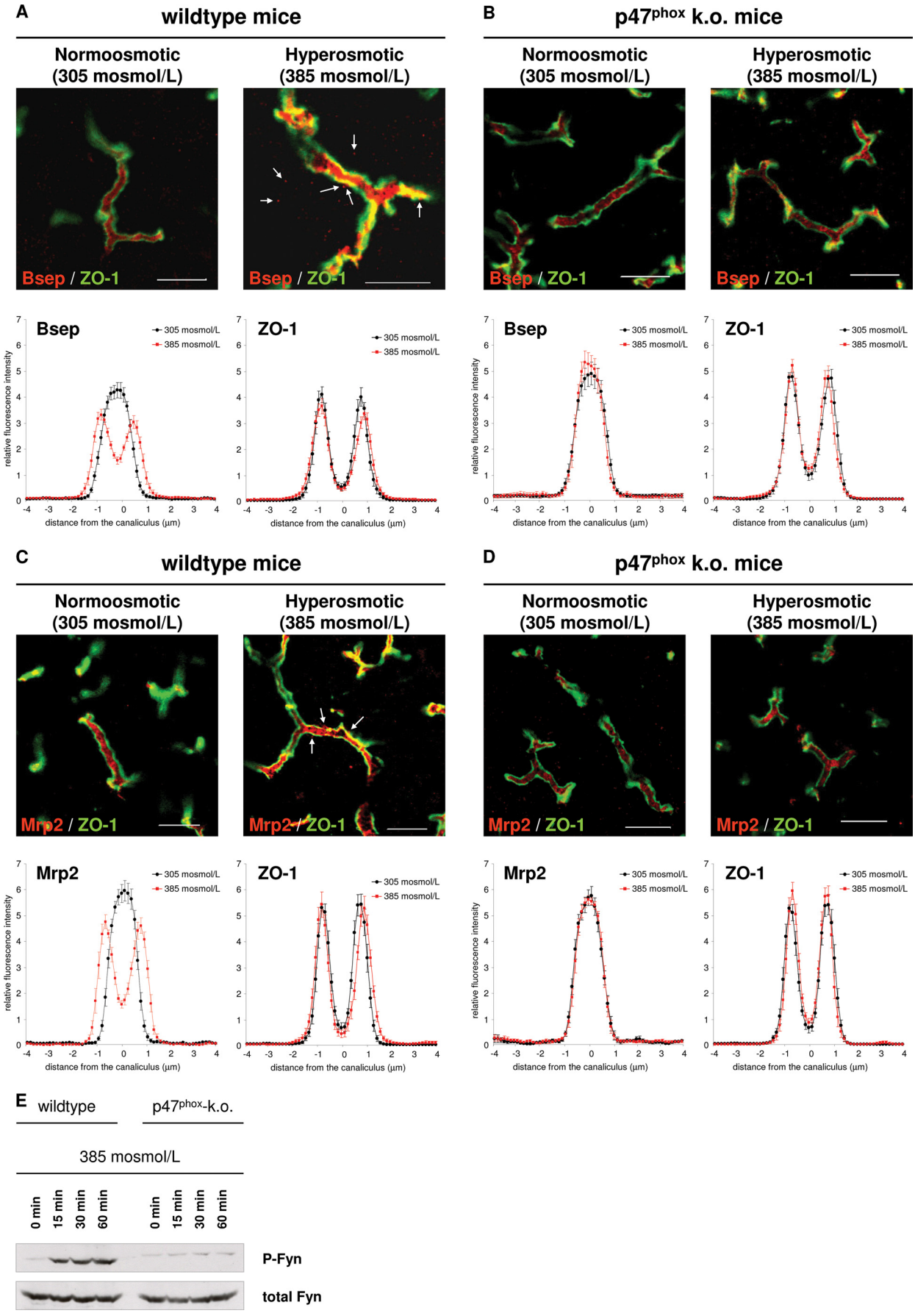
A
wildtype mice
Normoosmotic (305 mosmol/L)
Hyperosmotic (385 mosmol/L)
Bsep / ZO-1
B
p47phox k.o. mice
Normoosmotic (305 mosmol/L)
Hyperosmotic (385 mosmol/L)
Bsep / ZO-1
Bsep
ZO-1
305 mosmol/L
385 mosmol/L
relative fluorescence intensity
distance from the canaliculus (µm)
C
wildtype mice
Normoosmotic (305 mosmol/L)
Hyperosmotic (385 mosmol/L)
Mrp2 / ZO-1
D
p47phox k.o. mice
Normoosmotic (305 mosmol/L)
Hyperosmotic (385 mosmol/L)
Mrp2 / ZO-1
Mrp2
ZO-1
305 mosmol/L
385 mosmol/L
relative fluorescence intensity
distance from the canaliculus (µm)
E
wildtype
p47phox-k.o.
385 mosmol/L
0 min
15 min
30 min
60 min
0 min
15 min
30 min
60 min
P-Fyn
total Fyn

**TABLE 1**

**Effect of hyperosmolarity on CDNB-GS release into bile and effluent perfusate in the perfused rat liver**

CDNB (10 $\mu$mol/liter) was added to the influent perfusate after 30 min of normoosmolar (305 mosmol/liter) perfusion. If indicated, NAC (30 mmol/liter) was added after 50 min, and hyperosmolarity occurred after 60 min of perfusion. The concentrations of its glutathione conjugate (CDNB-GS) were determined in bile and effluent perfusate (mean ± S.E.; $n = 3$ for each condition). In condition A, hyperosmolarity (405 mosmol/liter) induced a significant decrease of CDNB-GS release into bile and a significant increase of CDNB-GS release into the effluent perfusate within 20 min, whereas for control total CDNB-GS release remained unchanged, indicating a hyperosmotic induced cholestasis ($p > 0.05$). In condition B, in the presence of NAC, hyperosmolarity-induced cholestasis was abolished as CDNB-GS release into bile, and effluent perfusate remained unchanged under these conditions. In condition C, as for control, NAC itself had no significant impact on both CDNB-GS release into bile or effluent perfusate.

| | Condition | CDNB-GS release | | |
|---|---|---|---|---|
| | | In bile | In perfusate | Total |
| | | *nmol/g liver/min* | | |
| A | Control | 50.5 ± 1.9 | 11.9 ± 0.7[a] | 62.4 ± 2.0 |
| | Hyperosmolarity (+50 mM NaCl) | 39.2 ± 2.1[a] | 21.8 ± 0.7[a] | 61.0 ± 2.3[b] |
| B | Control | 48.0 ± 0.6 | 14.5 ± 1.5 | 62.5 ± 1.8 |
| | NAC (30 mM) + hyperosmolarity | 49.7 ± 0.7[b.] | 16.3 ± 1.1[b.] | 66.0 ± 1.2[b] |
| C | Control | 50.3 ± 2.2 | 13.5 ± 1.0 | 63.8 ± 1.9 |
| | NAC (30 mM) + normoosmolarity | 51.4 ± 2.3[b] | 13.1 ± 1.6[b] | 64.5 ± 2.0[b] |

[a] $p < 0.05$.
[b] n.s., not significant.

ice and then centrifuged at 10,000 × *g* for 25 min at 4 °C, and aliquots were taken for protein determination using the Bio-Rad protein assay (Bio-Rad). The supernatants containing equal protein amounts (200 $\mu$g) were incubated for 2 h at 4 °C with a polyclonal rabbit anti-Yes or rabbit anti-Fyn antibody (dilution 1:100; Santa Cruz, CA) to immunoprecipitate Yes or Fyn, respectively. Then 10 $\mu$l of protein A and 10 $\mu$l of protein G-agarose (Santa Cruz, CA) was added and incubated at 4 °C overnight. Immunoprecipitates were washed 3 times with a buffer containing 136 mM NaCl, 20 mM Tris-HCl, 10% (v/v) glycerol, 2 mM EDTA, 50 mM $\beta$-glycerophosphate, 20 mM sodium pyrophosphate, 0.2 mM Pefablock, 5 $\mu$g/ml aprotinin, 5 $\mu$g/ml leupeptin, 4 mM benzamidine, 1 mM sodium vanadate, and 0.1% (v/v) Triton X-100 and then transferred to Western blot analysis as described above. The anti-phospho-Src family-Tyr-418 antibody was used to detect activating phosphorylation of Yes or Fyn in the respective immunoprecipitates (37).

*Analysis of CLF Transport in Rat Hepatocyte Couplets*—Rat hepatocyte couplets cultured on MaTek dishes were analyzed for CLF transport using an inverted fluorescence microscope (Zeiss, Axiovert) combined with the QuantiCell 2000-calcium imaging setup (VisiTech, Sunderland, UK). For fluorescence recording, cells were mounted with phenol red-free culture medium at 37 °C equilibrated with room atmosphere resulting in a pH of 7.4. Measurements of CLF fluorescence in hepatocyte couplets were performed simultaneously in the cytosol and the pseudocanaliculus by determination of the respective regions of interest using transmission microscopy and the QuantiCell 2000 software. Fluorescence measurements were then performed continuously at the excitation wavelength of 490 nm with a time resolution of 0.1 Hz by a monochromators, and emission was measured at 515–565 nm using a CCD camera as provided by the QuantiCell 2000-calcium imaging setup. The raw fluorescence signals were corrected for autofluorescence.

*Immunostaining of Rat Hepatocyte Couplets*—Rat hepatocyte couplets were isolated as described above and then grown on glass coverslips. After the respective stimulation, cells were fixed using Zamboni's fixative for 20 min at room temperature. After permeabilization in 0.1% Triton X-100 (2 min, 4 °C) and blocking by 5% FCS (30 min, room temperature), cells were incubated for 2 h with the following primary antibodies: rabbit anti-phospho-cortactin (diluted 1:50 in PBS) or mouse anti-cortactin (1:100 in PBS). Secondary antibodies were diluted 1:500 and if indicated mixed with phalloidin-FITC (1 $\mu$g/ml) and applied for 1 h at room temperature after intensive washing using PBS. Immunostained samples were then mounted in ProLong Gold antifade reagent with DAPI and analyzed using a Zeiss LSM 510 META confocal laser scanning system.

*Statistics*—Results from at least three independent experiments are expressed as the means ± S.E. *n* refers to the number of independent experiments. Results were analyzed using Student's *t* test. $p < 0.05$ was considered statistically significant.

## RESULTS

*Hyperosmolarity Induced Bsep and Mrp2 Retrieval from the Canalicular Membrane and Protein Kinase Activation in Perfused Rat Liver*—In line with previous data (17, 18), hyperosmolarity induced within 30 min a retrieval of both Bsep (Fig. 1*A*) and Mrp2 (Fig. 1*B*) from the canalicular membrane, suggestive for an osmo-dependent dynamic localization of the respective transporters, whereas localization of the tight junction protein ZO-1 remained unchanged (Fig. 1, *A* and *B*).

FIGURE 4. **Immunohistochemical distribution of Bsep (*A* and *B*) and Mrp2 (*C* and *D*) and Fyn activation in hyperosmotically perfused wild type (*A*, *C*, and *E*) and p47$^{phox}$ knock-out mouse liver (*B*, *D*, and *E*).** Mouse livers were perfused for 30 min with either normoosmotic (305 mosmol/liter; ■, *black graph*) or hyperosmolar Krebs-Henseleit buffer (385 mosmol/liter; ■, *red graph*) and immunostained for Bsep (*red*) and ZO-1 (*green*) (*A* and *B*) or for Mrp2 (*red*) and ZO-1 (*green*) (*C* and *D*), as described under "Experimental Procedures" and in the Fig. legend 1. The pictures refer to representative perfusion experiments. *White bar* = 10 $\mu$m. Under normoosmotic conditions, Bsep (*A* and *B*) and Mrp2 (*C* and *D*) are largely localized between the linear ZO-1 staining/tight junction complex, whereas after hyperosmotic perfusion Bsep ($A$, $p < 0.05$) and Mrp2 ($C$, $p < 0.05$) appear aside the linear ZO-1 staining/tight junction complex inside the cells in wild type animals (*A* and *C*) but remained unchanged in the p47$^{phox}$ knock-out mice (*k.o.*, *B* and *D*). The means of 40 measurements in each of the 3 individual experiments for each condition are shown (means ± S.E.). Statistical analysis was performed as described under "Experimental Procedures." *E*, in another set of experiments, livers from either wild type or p47$^{phox}$ knock-out mice were exposed to hyperosmotic medium (385 mosmol/liter), and liver samples were taken at the given time points. Fyn phosphorylation was detected by Western blot as described under "Experimental Procedures." Representative blots of three independent perfusion experiments per condition are shown. Fyn phosphorylation occurs within 15 min of hyperosmotic exposure in livers from wild type animals, whereas no Fyn activation occurred within 60 min in livers from p47$^{phox}$ knock-out mice, indicating an involvement of NADPH oxidase in hyperosmotic Fyn activation.

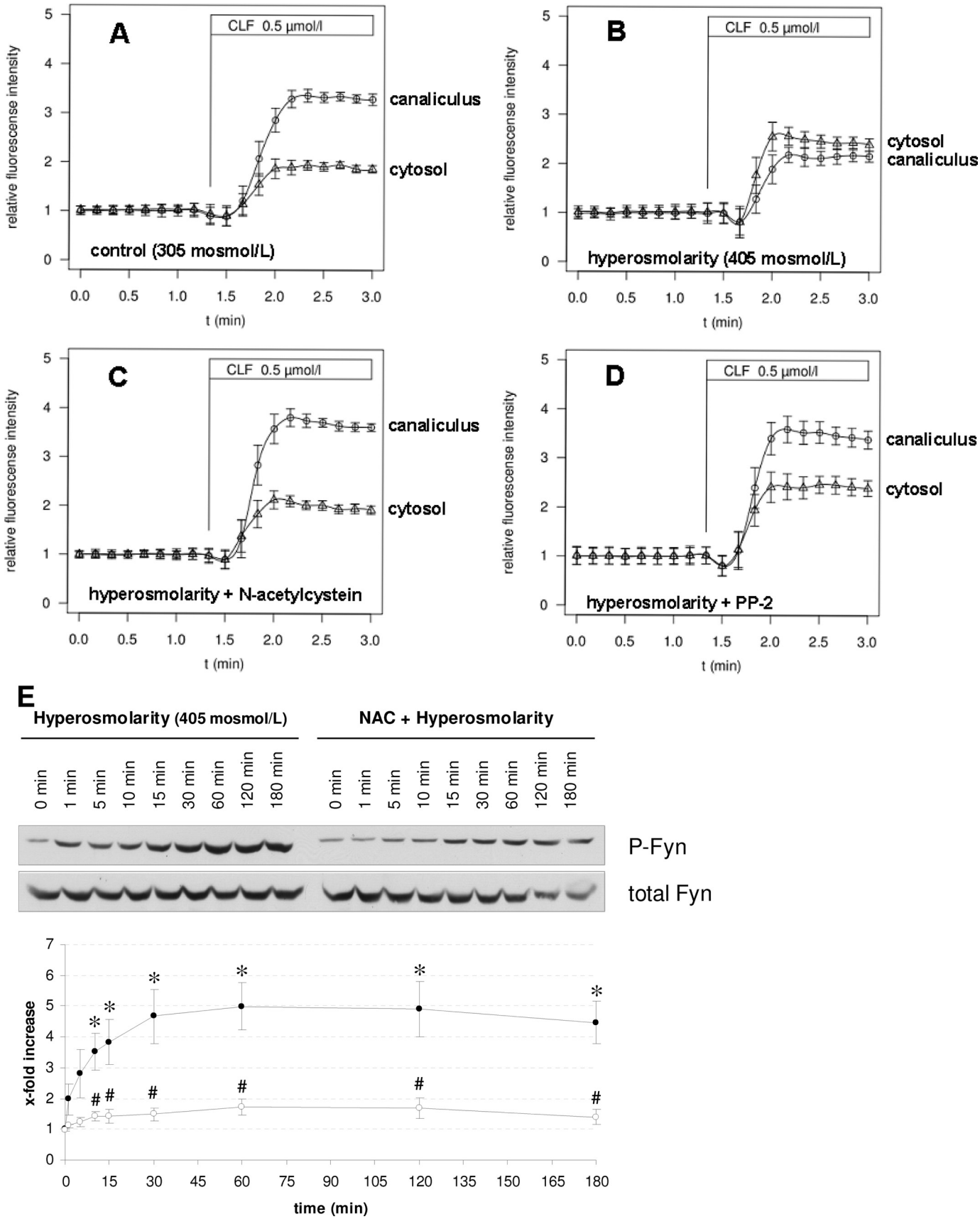
A
CLF 0.5 µmol/l
canaliculus
cytosol
control (305 mosmol/L)
relative fluorescense intensity
t (min)
B
CLF 0.5 µmol/l
cytosol
canaliculus
hyperosmolarity (405 mosmol/L)
C
CLF 0.5 µmol/l
canaliculus
cytosol
hyperosmolarity + N-acetylcystein
D
CLF 0.5 µmol/l
canaliculus
cytosol
hyperosmolarity + PP-2
E
Hyperosmolarity (405 mosmol/L)
NAC + Hyperosmolarity
0 min
1 min
5 min
10 min
15 min
30 min
60 min
120 min
180 min
P-Fyn
total Fyn
x-fold increase
time (min)

As shown recently (26), hyperosmotic exposure of primary rat hepatocytes led within 30 min to an activation of the Src family kinases Yes and Fyn, whereas no c-Src activation became detectable within 180 min of hyperosmotic exposure. A similar behavior of Src family kinases was also found in the intact perfused rat liver in response to hyperosmotic perfusion (this study). Fig. 2*A* depicts the perfusion plan chosen for these experiments. As shown in Fig. 2*B*, hyperosmolarity induced within 30 min an activating phosphorylation of Yes and Fyn but not of c-Src. NADPH oxidase-driven ROS formation mediates the hyperosmotic Src kinase activation in primary rat hepatocytes, as demonstrated recently by inhibitor studies (*i.e.* apocynin, neopterin, DPI), $p47^{phox}$-siRNA approaches, and experiments with $p47^{phox}$-knock-out mice (25). Also apocynin, a NADPH oxidase inhibitor, and the antioxidant NAC strongly blunted the hyperosmolarity-induced Yes and Fyn activation in perfused rat liver, suggestive for a NADPH oxidase-driven and ROS-dependent activation of Yes and Fyn (Fig. 2*B*). In addition, also the Src kinase inhibitors SU6656 (38) and PP-2 (39) were tested. Both compounds are known to inhibit Fyn, whereas Yes is inhibited only by SU6656 but not by PP-2 (26, 39). This was confirmed in this study; SU6656 inhibited both hyperosmotic Yes and Fyn activation, whereas PP-2 inhibited Fyn but not Yes phosphorylation upon hyperosmotic exposure in the perfused rat liver (Fig. 2*B*). Although SU6656 and PP-2 may also inhibit c-kit and abl, an involvement of these kinases is unlikely because both kinases may be found in hepatocellular tumors or in the regenerating liver but are not expressed in normal hepatocytes (40, 41).

In addition to Src kinases, also the MAP kinases Erk, $p38^{MAPK}$, and JNK are regulated by anisoosmolarity as shown in primary rat hepatocytes (21, 23). Thus, liver samples were also detected for hyperosmolarity-induced MAP kinase phosphorylation. Hyperosmolarity induced within 30 min an activation of JNK, which was sensitive to inhibition of NADPH oxidase by apocynin and the anti-oxidant NAC, whereas the Src kinase inhibitors SU6656 and PP-2 were ineffective (Fig. 2*C*). These data suggest that hyperosmotic JNK activation is mediated by a NADPH oxidase-driven ROS formation and does not require Fyn or Yes activation. Time courses for the hyperosmotic phosphorylation of Src and MAP kinases in perfused rat liver are given in supplemental Fig. 1.

*Pharmacological Characterization of the Hyperosmolarity-induced Retrieval of Bsep and Mrp2 from the Canalicular Membrane in Perfused Rat Liver*—As shown in Fig. 3, apocynin (Fig. 3*A*) and NAC (Fig. 3*B*) inhibited hyperosmolarity-induced Bsep (Fig. 3) and Mrp2 (see supplemental Fig. 2, *A–C*) retrieval from the canalicular membrane, whereas ZO-1 distribution remained unchanged, pointing to a role of NADPH oxidase-driven ROS formation in triggering transporter retrieval. Also, the Src kinase inhibitors SU6656 (Fig. 3*C*) and PP-2 (Fig. 3*D*) abolished the hyperosmolarity-induced Bsep (Fig. 3) and Mrp2 (see supplemental Fig. 2, *A*, *D*, and *E*) retrieval from the canalicular membrane. Because PP-2 inhibits hyperosmotic Fyn but not Yes activation (Fig. 2*A*), these findings suggest that Fyn, but not Yes, is involved in the hyperosmotic Bsep and Mrp2 retrieval from the canalicular membrane.

A role of JNK in mediating the hyperosmotic Bsep and Mrp2 retrieval from the canalicular membrane was ruled out by the findings that two different JNK inhibitors, *i.e.* L-JNKI-1 (100 nmol/liter) (42) and SP600125 (10 $\mu$mol/liter) (43), had no effect on the hyperosmolarity-induced Bsep and Mrp2 retrieval from the canalicular membrane (not shown). It should be noted that all inhibitors used in this study, *i.e.* apocynin, NAC, SU6656, PP-2, L-JNKI-1, and SP600125 had themselves no effect on Bsep or Mrp2 localization (see supplemental Fig. 3).

*Hyperosmolarity-induced Bsep and Mrp2 Retrieval from the Canalicular Membrane Is Blunted in $p47^{phox}$ Knock-out Mouse*—To further elucidate the critical role of NADPH oxidase in hyperosmotically induced Bsep and Mrp2 retrieval from the canalicular membrane, livers from $p47^{phox}$ knock-out mice were perfused with either hyperosmotic or hyperosmotic medium, and transporter localization was investigated by immunohistochemistry.

As shown in Fig. 4, hyperosmolarity induced within 30 min a retrieval of both Bsep (Fig. 4*A*) and Mrp2 (Fig. 4*C*) from the canalicular membrane of wild type mice, whereas no retrieval of Bsep (Fig. 4*B*) or Mrp2 (Fig. 4*D*) was detectable in livers from $p47^{phox}$ knock-out mice. In addition, within 60 min no Fyn activation occurred in the perfused liver of $p47^{phox}$ knock-out mice, whereas Fyn activation became detectable within 15 min in wild type animals (Fig. 4*E*). Therefore, NADPH oxidase isoform activation is a critical step in hyperosmolarity-induced Fyn activation and Bsep and Mrp2 retrieval from the canalicular membrane.

*Functional Relevance of the Hyperosmolarity-induced Transporter Retrieval from Canalicular Membrane in Perfused Rat Liver and Primary Rat Hepatocyte Couplets*—As shown in Table 1 and Fig. 5, the hyperosmolarity-induced Mrp2 retrieval was accompanied by an inhibition of canalicular secretion. Rat livers were perfused with CDNB, and the concentrations of its glutathione conjugate (CDNB-GS), which is a Mrp2 substrate,

FIGURE 5. **Hyperosmolarity-induced decrease of CLF transport into pseudocanaliculi and NAC sensitivity of Fyn activation in primary rat hepatocyte couplets.** Primary rat hepatocyte couplets were prepared and cultured as described under "Experimental Procedures." *A–D*, at the beginning of the experiment, normoosmotic (305 mosmol/liter) or hyperosmotic medium (405 mosmol/liter) was instituted for 30 min. When indicated, NAC (30 mM) or PP-2 (5 $\mu$M) was added to the medium for 30 min. Thereafter, hepatocyte couplets were transferred to an inverted fluorescence microscope and challenged with the fluorescent bile salt derivative CLF (0.5 $\mu$mol/liter). CLF fluorescence was continuously monitored in the cytosol (△ and the pseudocanaliculus (○) formed by the hepatocyte couplet. Mean fluorescence during the first minute of recording was set to 1. Data are given as the means ± S.E. ($n = 3$ for each condition). *A*, under normoosmotic conditions, CLF accumulates predominantly in the pseudocanaliculus. *B*, under hyperosmotic conditions, the amount of CLF in the pseudocanaliculus decreases compared with normoosmotic control, whereas CLF fluorescence in the cytosol is increased. *C* and *D*, hyperosmolarity-induced decrease of CLF transport into the pseudocanaliculus was abolished in the presence of either NAC (*C*) or PP-2 (*D*), suggesting an involvement of ROS and Src kinases in this setting. *E*, hepatocyte couplets were exposed to hyperosmolarity (405 mosmol/liter) for the indicated time periods. When indicated, NAC (30 mM) was present for 30 min before institution of hyperosmolarity. Activation of Fyn was analyzed densitometrically as described under "Experimental Procedures." Respective Blots of three independent experiments are given. Hyperosmolarity induced within 10 min a significant Fyn phosphorylation that lasted for up to 180 min (*, $p < 0.05$, $n = 3$). This hyperosmotic Fyn activation in 6-h-cultured rat hepatocyte couplets was significantly inhibited by NAC (#, $p < 0.05$, $n = 3$).

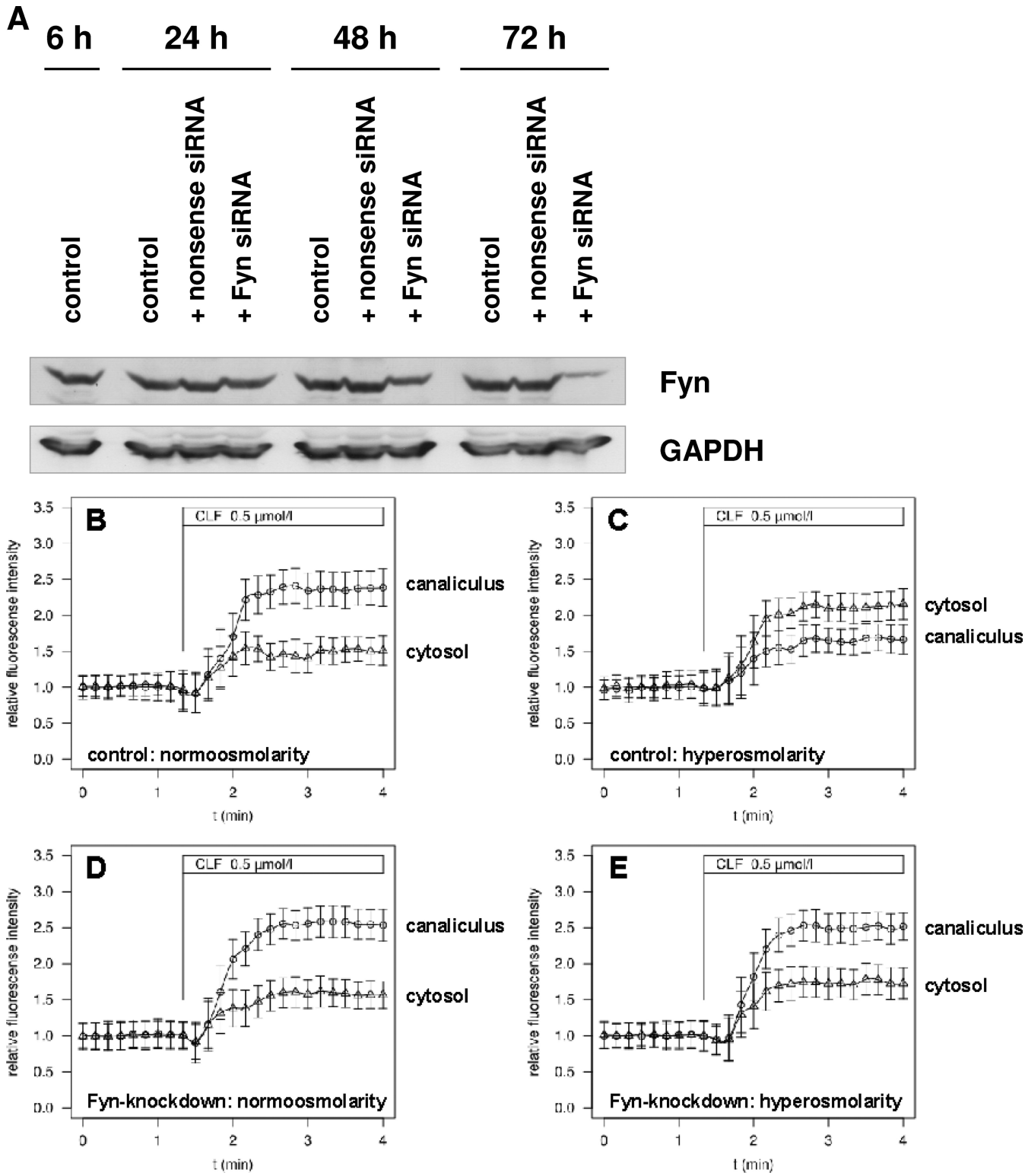


FIGURE 6. **Hyperosmolarity-induced decrease of CLF transport into pseudocanaliculi is blunted in primary rat hepatocyte couplets after Fyn knockdown.** Primary rat hepatocyte couplets were isolated, kept in culture, and treated with either nonsense (*A*, *B*, and *C*; *control*) or Fyn siRNA for 72 h (*A*, *D*, and *E*; Fyn knockdown) as described under "Experimental Procedures." Measurements were performed as described in the Fig. 5 legend. CLF fluorescence was continuously monitored in the cytosol (△) and the pseudocanaliculus (○) formed by the hepatocyte couplet. Mean fluorescence during the first minute of recording was set as 1. Data are given as the means ± S.E. ($n = 3$ for each condition). *A*, Fyn knockdown was achieved after 72 h of Fyn siRNA treatment, whereas Fyn expression remained unchanged in hepatocyte couplets exposed to nonsense siRNA as detected by Western blot. GAPDH served as a loading control and was not affected by Fyn siRNA treatment. Representative blots of three independent experiments are shown. *B* and *C*, in control cells, CLF accumulates predominantly in the pseudocanaliculus under normoosmotic conditions (*B*, 305 mosmol/liter), whereas hyperosmolarity (*C*, 405 mosmol/liter) decreases CLF fluorescence in the pseudocanaliculus when compared with the normoosmotic control condition and increases CLF fluorescence in the cytosol. *D* and *E*, in hepatocyte couplets with Fyn knockdown, the hyperosmolarity-induced decrease of CLF transport into the pseudocanaliculus was abolished (*E*) compared with normoosmotic conditions (*D*).

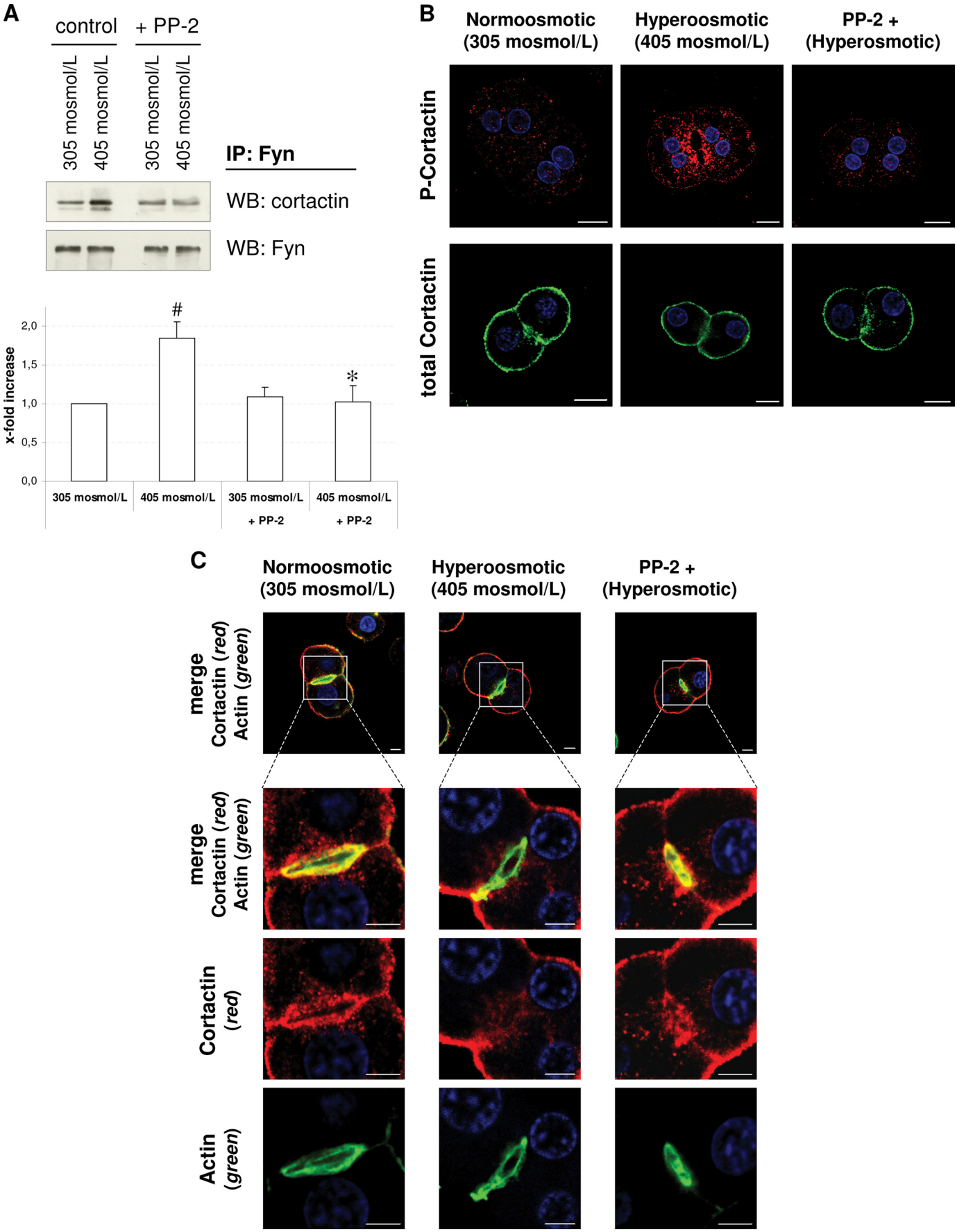
A
control
+ PP-2
305 mosmol/L
405 mosmol/L
305 mosmol/L
405 mosmol/L
IP: Fyn
WB: cortactin
WB: Fyn
x-fold increase
2,0
1,5
1,0
0,5
0,0
#
*
305 mosmol/L
405 mosmol/L
305 mosmol/L + PP-2
405 mosmol/L + PP-2
B
Normoosmotic (305 mosmol/L)
Hyperoosmotic (405 mosmol/L)
PP-2 + (Hyperosmotic)
P-Cortactin
total Cortactin
C
Normoosmotic (305 mosmol/L)
Hyperoosmotic (405 mosmol/L)
PP-2 + (Hyperosmotic)
merge Cortactin (red) Actin (green)
merge Cortactin (red) Actin (green)
Cortactin (red)
Actin (green)

were determined in bile and the effluent perfusate. As shown in Table 1, condition A, hyperosmolarity induced within 20 min a significant decrease of CDNB-GS release into bile and a corresponding increase of CDNB-GS release into the effluent perfusate. Total CDNB-GS release remained unaffected, indicating that hyperosmolarity did not interfere with the CDNB conjugation process. In the presence of NAC, the hyperosmolarity-induced inhibition of CDNB-GS secretion into bile was no longer detectable (Table 1, condition B). NAC itself had no effect on CDNB-GS release into bile or effluent perfusate (Table 1, condition C). These findings suggest that the antioxidant NAC not only prevents hyperosmotic Fyn activation and Mrp2 retrieval from the canalicular membrane but also the inhibition of Mrp2 substrate secretion into bile.

Primary rat hepatocyte couplets were further tested for transport of the fluorescent bile salt derivative CLF, a known OATP1B3 and Mrp2 substrate (44). CLF fluorescence was continuously monitored in the cytosol and the pseudocanaliculus formed by a hepatocyte couplet. As shown in Fig. 5*A*, CLF rapidly accumulated in the pseudocanaliculus under normoosmotic conditions, thereby exceeding the CLF fluorescence retained inside the hepatocytes under steady state conditions and indicating that Mrp2 is able to build up an CLF concentration gradient. Under hyperosmotic conditions, however, the amount of CLF in the pseudocanaliculus was decreased, whereas CLF fluorescence in the cytosol was increased (Fig. 5*B*). This hyperosmolarity-induced decrease in CLF transport into the pseudocanaliculus was prevented in the presence of NAC (Fig. 5*C*) or PP-2 (Fig. 5*D*). Due to their autofluorescence, which interfered with the CLF fluorescence measurements, apocynin and SU6656 could not be studied in this setting.

Because NAC was able to inhibit the hyperosmolarity-induced decrease in CLF transport to the pseudocanaliculus (Fig. 5*C*), it was tested whether NAC inhibits hyperosmolarity-induced Fyn activation in hepatocyte couplets. As shown in Fig. 5*E*, hyperosmolarity induced within 10 min a significant Fyn phosphorylation that lasted for up to 180 min (*, $p < 0.05$, $n = 3$). This hyperosmotic Fyn activation in 6-h-cultured rat hepatocyte couplets was significantly inhibited by NAC (#, $p < 0.05$, $n = 3$). In line with previous studies (27), hyperosmolarity induced within 30 min a Fyn activation in 24-h-cultured rat hepatocytes (*, $p < 0.05$, $n = 3$), which, however, was insensitive toward NAC ($p > 0.05$, $n = 3$) (see supplemental Fig. 4). The reason for this discrepancy between 6-h-cultured rat hepatocyte couplets and 24-h-cultured rat hepatocytes is unclear but may relate to differences in culture time and/or cell polarization.

To strengthen the critical role of Fyn in hyperosmotically induced cholestasis, a Fyn knockdown approach using siRNA was performed in rat hepatocyte couplets. A significant Fyn knockdown was achieved within 72 h of siRNA treatment, whereas no change in Fyn expression occurred in hepatocyte couplets treated with nonsense siRNA (Fig. 6*A*). Again, CLF measurements were performed that showed a hyperosmolarity-induced decrease of CLF transport into the pseudocanaliculi compared with hyperosmotic osmolarity in the control cells (*i.e.* nonsense siRNA, Fig. 6, *B* and *C*), whereas the hyperosmolarity effect was largely abolished after Fyn knockdown (*i.e.* Fyn siRNA, Fig. 6, *D* and *E*).

*Cortactin as a Downstream Target of Hyperosmotic Fyn Activation*—In rat hepatocyte couplets, oxidative stress-mediated Bsep internalization is accompanied by a derangement of the actin cytoskeleton (45), and in fibroblasts hyperosmolarity can induce a Fyn-mediated phosphorylation of the actin-binding protein cortactin (46), which results in a reduction of its F-actin cross-linking activity (47). Thus, cortactin might be a potential downstream target of Fyn, which participates in the hyperosmotic transporter retrieval from the canalicular membrane. Therefore, it was tested in rat hepatocyte couplets whether hyperosmolarity induces an association between Fyn and cortactin, resulting in cortactin phosphorylation near the canalicular membrane.

As shown by Fyn co-immunoprecipitation studies (Fig. 7*A*), hyperosmolarity induced within 30 min a significant and PP-2 (5 $\mu$mol/liter)-sensitive Fyn/cortactin association ($n = 5$, $p < 0.05$) suggestive for an interaction of both proteins. Furthermore, within 30 min of hyperosmotic exposure (405 mosmol/liter) there was a PP-2 (5 $\mu$mol/liter)-sensitive increase of phosphorylated cortactin mainly at the peri-pseudocanalicular region (Fig. 7*B*). In line with the literature (47), phosphorylation of cortactin is accompanied by a reduction of actin/cortactin association as visualized by phalloidin-FITC/cortactin costaining (Fig. 7*C*). With respect to confocal laser-scanning microscopy, the hyperosmolarity-induced and PP-2-sensitive decrease in phalloidin-FITC/cortactin association was mainly observed at the pseudocanaliculi formed by the hepatocyte couplets (Fig. 7*C*). These data suggest that cortactin is a downstream target of hyperosmolarity-induced Fyn activation and represents a likely candidate that is involved in the Fyn-mediated Bsep and Mrp2 retrieval from the canalicular membrane.

FIGURE 7. **Hyperosmolarity-induced Fyn/cortactin association (*A*), cortactin tyrosine phosphorylation (*B*), and reduction of cortactin/actin association (*C*) in rat hepatocytes.** Primary rat hepatocytes (*A*) or hepatocyte couplets (*B* and *C*) were isolated and cultured as described under "Experimental Procedures." At the beginning of the experiment, normoosmotic (305 mosmol/liter) or hyperosmotic medium (405 mosmol/liter) was instituted for 30 min. When indicated, PP-2 (5 $\mu$mol/liter) was added to the medium for 30 min. At the end of the experiment cells were either transferred for Fyn immunoprecipitation (*A*) or to immunostaining of either phospho-cortactin-Tyr-421 (*red*) or total cortactin (*green*) (*B*) or total cortactin (*red*) and phalloidin-FITC (*green*), respectively, to visualize the actin cytoskeleton (*C*). Cell nuclei were stained using DAPI (*blue*) (*B* and *C*). *A*, after Fyn immunoprecipitation (*IP*), samples were tested for Fyn/cortactin association by cortactin Western blot (*WB*). Fyn Western blots served as loading controls. Hyperosmolarity led within 30 min to a significant increase in Fyn/cortactin association ($n = 5$, $p < 0.05$) that was sensitive to PP-2 ($n = 5$, $p < 0.05$). *B*, compared with normoosmotic control (*left column*), hyperosmolarity (*middle column*) induces a PP-2-sensitive increase in cortactin tyrosine phosphorylation (*upper row*), whereas total cortactin remains unchanged (*lower row*) ($n = 5$). *White bar* = 10 $\mu$m. *C*, whereas a strong colocalization of cortactin and actin was visible under normoosmotic conditions, hyperosmolarity induced a dissociation of cortactin and actin mainly at the pseudocanalicular region in a PP-2-sensitive way. Representative immunostainings of three independent experiments are shown ($n = 3$). The *upper lane* represents a low magnification showing the respective hepatocyte couplet (*white bar* = 5 $\mu$m). The three lower lanes show a confocal section of the pseudocanaliculus (*white bar* = 5 $\mu$m).

## DISCUSSION

As shown previously, short term regulation of the bile salt export pump Bsep (18) and multidrug resistance protein Mrp2 (17) by ambient osmolarity occurs at the level of transporter insertion/retrieval into/from the canalicular membrane in addition to a long term osmo-regulation of transporter gene expression (15). Under normoosmotic conditions, Bsep and Mrp2 are found in both the canalicular membrane and in putative transporter-containing vesicles in the subcanalicular area of the hepatocyte (17, 18, 46). Hyperosmolarity increases the fraction of Bsep and Mrp2, which is located inside the hepatocytes, whereas hypoosmolarity favors the insertion of intracellular Bsep and Mrp2 into the canalicular membrane (17, 18, 48). These osmo-dependent shifts in Bsep and Mrp2 location occur within less than 30 min and are reversible, suggesting the existence of a dynamic subcanalicular Bsep and Mrp2 pool, which can be recruited to the canalicular membrane in response to cell swelling (17, 18, 48) and which enlarges in response to cell shrinkage due to transporter retrieval from the canalicular membrane (17, 18). The osmo-sensing and -signaling pathways that mediate the hypoosmotic increase of taurocholate excretory capacity in perfused rat liver involve an integrin-mediated activation of the focal adhesion kinase and c-Src (50) followed by a dual activation of the mitogen-activated protein kinases Erk and $p38^{MAPK}$ and a downstream microtubule-dependent mechanism (15, 16, 49). It is likely that these osmo-signaling events also govern the insertion of immunoreactive Bsep and Mrp2 into the canalicular membrane in response to hepatocyte swelling. The signaling events that trigger the hyperosmotic Bsep and Mrp2 retrieval and decrease of taurocholate excretory capacity were investigated in this study.

NADPH oxidase activation was shown to occur in response to cell shrinkage by either hyperosmolarity (25) or hydrophobic bile acids (50) and, as shown this study, may trigger the retrieval of Bsep and Mrp2 from the canalicular membrane. In line with this, the hyperosmolarity-induced Bsep/Mrp2 retrieval from the canalicular membrane was sensitive to inhibition of the oxidative stress response by apocynin or the antioxidant *N*-acetylcysteine and was also largely abolished in livers from $p47^{phox}$ knock-out mice. Furthermore, NAC also prevented the hyperosmolarity-induced inhibition of cholyl-lysyl-fluorescein secretion in hepatocyte couplets or of the CDNB-conjugate excretion into bile in liver perfusion experiments.

Hyperosmotic ROS formation was shown to trigger an activation of the Src kinases Yes and Fyn (26). Hyperosmolarity-induced Yes phosphorylation mediates EGFR transactivation (26), which is required for EGFR-driven CD95 tyrosine phosphorylation (24), a crucial step in hyperosmotic induction of apoptosis, whereas Fyn does not participate here. As shown in this study, hyperosmotic Fyn activation triggers transporter retrieval from the canalicular membrane. In line with this, PP-2, which blocks the hyperosmotic phosphorylation of Fyn but not of Yes, abolished hyperosmotic Bsep/and Mrp2 internalization. Likewise, inhibitors of the upstream events leading to hyperosmotic Fyn activation, such as apocynin or NAC, prevented hyperosmotic transporter internalization. Furthermore, Fyn knockdown in hepatocyte couplets abolished the hyperosmotic inhibition of CLF secretion into the pseudocanaliculi, and in $p47^{phox}$ knock-out mice both hyperosmolarity-induced Fyn activation and transporter retrieval were largely inhibited.

These data strongly suggest that Fyn mediates the hyperosmolarity-induced Bsep and Mrp2 retrieval from the canalicular membrane and cholestasis. So far little is known about the function of Fyn in liver. In NIH 3T3 and 293 cells evidence has been presented that the hepatitis B virus HBx protein can activate the Ras-Raf-MAP kinase pathway via Fyn (51). In addition, Fyn was shown to be involved in angiotensin II-induced and Raf-1-mediated mitogenic pathways in liver epithelial cells (52). This study identifies ROS-mediated Fyn activation as a crucial step in canalicular bile acid transporter retrieval and subsequent cholestasis. It is an interesting question whether Fyn is also involved in the Mrp2 and/or Bsep retrieval induced by endotoxin (53), hydroperoxides (54), bile duct ligation (55), or estradiol-17$\beta$-D-glucuronide (56).

$Fyn^{-/-}$ knock-out mice exhibit a lower adipocyte cell size and an improved peripheral tissue insulin sensitivity (57). In addition, hepatic steatosis induced by chronic ethanol consumption is reduced in $Fyn^{-/-}$ knock-out mice and accompanied by a decrease in hepatic free fatty acid and triglyceride levels compared with wild type mice (58). Bile acids were recently described to influence glucose homeostasis, lipid metabolism, and energy expenditure via the bile acid membrane receptor TGR5 (59). It is an open question to what extent Fyn-mediated changes in bile acid handling contribute to these metabolic effects.

JNK activation is crucial for the hyperosmotic activation of CD95-dependent apoptosis (23, 24) but is apparently not involved in the hyperosmolarity-induced cholestasis. This is evidenced by the findings that neither PP-2, an inhibitor of Src family kinases c-Src and Fyn, nor SU6656, an inhibitor of Yes, Fyn, and c-Src, affected hyperosmotic JNK activation, whereas these inhibitors prevented the hyperosmotic retrieval of Bsep and Mrp2 from the canalicular membrane. Whereas Fyn mediates hyperosmotic Bsep and Mrp2 retrieval from the canalicular membrane in response to hyperosmotic cell shrinkage, hypoosmotic hepatocyte swelling triggers choleresis via activation of c-Src (49). Thus, different Src kinase family members are involved in mediating the response to osmotic hepatocyte swelling and shrinkage.

The $Na^+$/taurocholate cotransport polypeptide (Ntcp) was shown to translocate to the basolateral membrane upon cell swelling induced by hypoosmolarity in a PI 3-kinase- and cAMP-dependent way (60), whereas conventional $Ca^{2+}$-dependent protein kinase C isoforms can trigger Ntcp endocytosis, which may protect hepatocytes from toxic intracellular bile salt concentrations (61). It remains to be investigated whether hyperosmolarity also triggers Ntcp retrieval from the basolateral membrane and whether this is mediated by Fyn. Also the role of Fyn in the long term regulation of bile acid transporters requires investigation because hyperosmolarity was shown to down-regulate Bsep mRNA in cultured rat hepatocytes (11).

The molecular mechanisms underlying the Fyn-mediated transporter retrieval from the canalicular membrane remain unclear. However, as shown in this study, hyperosmolarity triggers a PP-2-sensitive Fyn/cortactin association, an accumula-

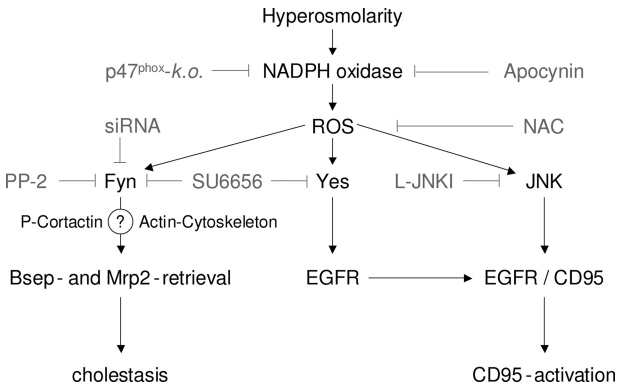


FIGURE 8. **Hyperosmolarity-induced Bsep and Mrp2 retrieval out of the canalicular membrane requires NADPH oxidase-driven ROS formation and subsequent Fyn activation.** Fig, 6 summarizes our findings. Hyperosmolarity-induced Yes, Fyn, and JNK activation were sensitive to inhibition of NADPH oxidase and to the antioxidant NAC, indicating an involvement of NADPH oxidase-driven ROS formation in the hyperosmotic Yes, Fyn, and JNK activation. PP-2 inhibits hyperosmotic Fyn but not Yes and JNK activation. Fyn then mediates the hyperosmotic-induced retrieval of canalicular Bsep and Mrp2. ROS-mediated Yes activation leads to an EGFR transactivation (26). JNK, which is also activated by hyperosmolarity, then provides a signal for EGFR/CD95 association and subsequent CD95 tyrosine phosphorylation followed by CD95 membrane translocation and DISC (death-inducing signaling complex) formation (24, 26). Therefore, Yes and JNK play a crucial role in hyperosmolarity-induced CD95 activation, whereas Fyn triggers cholestasis. *k.o.*, knock-out.

tion of phosphorylated cortactin underneath the canalicular membrane, and a reduction of cortactin/actin association (Fig. 7). A hyperosmolarity-induced and Fyn-mediated phosphorylation of the actin-binding protein cortactin had already been described in fibroblasts (46). Phosphorylated cortactin was shown to exhibit a diminished F-actin cross-linking activity (47) and a cytoskeletal F-actin disarrangement, which accompanied the oxidative stress-mediated Bsep internalization in rat hepatocyte couplets (45). Thus, one is tempted to speculate that the hyperosmotic Fyn activation interferes with the actin cytoskeleton in a way that favors transporter retrieval from the canalicular membrane. Further studies are required to strengthen this hypothesis. Fig. 8 schematically summarizes our current view on hyperosmotic signaling toward cholestasis.

*Acknowledgments—We gratefully acknowledge the excellent technical assistance of Nicole Eichhorst and Elisabeth Winands.*

## REFERENCES


1. Keppler, D., and Konig, J. (1997) *FASEB J.* **11,** 509–516
2. Gatmaitan, Z. C., and Arias, I. M. (1995) *Physiol. Rev.* **75,** 261–275
3. Müller, M., and Jansen, P. L. (1997) *Am. J. Physiol.* **272,** 1285–1303
4. Meier, P. J. (1995) *Am. J. Physiol.* **268,** 801–812
5. Vos, T. A., Hooiveld, G. J., Koning, H., Childs, S., Meijer, D. K., Moshage, H., Jansen, P. L., and Müller, M. (1998) *Hepatology* **28,** 1637–1644
6. Trauner, M., Arrese, M., Lee, H., Boyer, J. L., and Karpen, S. J. (1998) *J. Clin. Invest.* **15,** 2092–2100
7. Kubitz, R., Wettstein, M., Warskulat, U., and Häussinger, D. (1999) *Gastroenterology* **116,** 401–410
8. Demeule, M., Jodoin, J., Beaulieu, E., Brossard, M., and Béliveau, R. (1999) *FEBS Lett.* **442,** 208–214
9. Koopen, N. R., Wolters, H., Havinga, R., Vonk, R. J., Jansen, P. L., Müller, M., and Kuipers, F. (1998) *Hepatology* **27,** 537–545
10. Kubitz, R., Warskulat, U., Schmitt, M., and Häussinger, D. (1999) *Biochem. J.* **340,** 585–591
11. Warskulat, U., Kubitz, R., Wettstein, M., Stieger, B., Meier, P. J., and Häussinger, D. (1999) *Biol. Chem.* **380,** 1273–1279
12. Schliess, F., Kurz, A. K., vom Dahl, S., and Häussinger, D. (1997) *Gastroenterology* **113,** 1306–1314
13. Bruck, R., Haddad, P., Graf, J., and Boyer, J. L. (1996) *Am. J. Physiol.* **262,** 806–812
14. Häussinger, D., Hallbrucker, C., Saha, N., Lang, F., and Gerok, W. (1992) *Biochem. J.* **288,** 681–689
15. Häussinger, D., Saha, N., Hallbrucker, C., Lang, F., and Gerok, W. (1993) *Biochem. J.* **291,** 355–360
16. Noé, B., Schliess, F., Wettstein, M., Heinrich, S., and Häussinger, D. (1996) *Gastroenterology* **110,** 858–865
17. Kubitz, R., D'urso, D., Keppler, D., and Häussinger, D. (1997) *Gastroenterology* **113,** 1438–1442
18. Schmitt, M., Kubitz, R., Lizun, S., Wettstein, M., and Häussinger, D. (2001) *Hepatology* **33,** 509–518
19. Häussinger, D. (1996) *Biochem. J.* **313,** 697–710
20. Lang, F., Busch, G. L., Ritter, M., Völkl, H., Waldegger, S., Gulbins, E., and Häussinger, D. (1998) *Physiol. Rev.* **78,** 247–306
21. vom Dahl, S., Schliess, F., Reissmann, R., Görg, B., Weiergräber, O., Kocalkova, M., Dombrowski, F., and Häussinger, D. (2003) *J. Biol. Chem.* **278,** 27088–27095
22. Reinehr, R., Sommerfeld, A., and Häussinger, D. (2010) *J. Biol. Chem.* **285,** 25904–25912
23. Reinehr, R., Graf, D., Fischer, R., Schliess, F., and Häussinger, D. (2002) *Hepatology* **36,** 602–614
24. Reinehr, R., Schliess, F., and Häussinger, D. (2003) *FASEB J.* **17,** 731–733
25. Reinehr, R., Becker, S., Braun, J., Eberle, A., Grether-Beck, S., and Haüssinger, D. (2006) *J. Biol. Chem.* **281,** 23150–23166
26. Reinehr, R., Becker, S., Höngen, A., and Haüssinger, D. (2004) *J. Biol. Chem.* **279,** 23977–23987
27. Thomas, S. M., and Brugge, J. S. (1997) *Annu. Rev. Cell Dev. Biol.* **13,** 513–609
28. Bjorge, J. D., Jakymiw, A., and Fujita, D. J. (2000) *Oncogene* **19,** 5620–5635
29. Gerloff, T., Stieger, B., Hagenbuch, B., Madon, J., Landmann, L., Roth, J., Hofmann, A. F., and Meier, P. J. (1998) *J. Biol. Chem.* **273,** 10046–10050
30. Büchler, M., König, J., Brom, M., Kartenbeck, J., Spring, H., Horie, T., and Keppler, D. (1996) *J. Biol. Chem.* **271,** 15091–15098
31. Stevenson, B. R., Siliciano, J. D., Mooseker, M. S., and Goodenough, D. A. (1986) *J. Cell Biol.* **103,** 755–766
32. Graf, J., Gautam, A., and Boyer, J. L. (1984) *Proc. Natl. Acad. Sci. U.S.A.* **81,** 6516–6520
33. Sies, H. (1978) *Methods Enzymol.* **52,** 48–59
34. vom Dahl, S., Hallbrucker, C., Lang, F., and Häussinger, D. (1991) *Biochem. J.* **280,** 105–109
35. Wahlländer, A., and Sies, H. (1979) *Eur. J. Biochem.* **96,** 441–446
36. Akerboom, T. P., and Sies, H. (1989) *Methods Enzymol.* **173,** 523–534
37. Piiper, A., Elez, R., You, S. J., Kronenberger, B., Loitsch, S., Roche, S., and Zeuzem, S. (2003) *J. Biol. Chem.* **278,** 7065–7072
38. Blake, R. A., Broome, M. A., Liu, X., Wu, J., Gishizky, M., Sun, L., and Courtneidge, S. A. (2000) *Mol. Cell. Biol.* **20,** 9018–9027
39. Hanke, J. H., Gardner, J. P., Dow, R. L., Changelian, P. S., Brissette, W. H., Weringer, E. J., Pollok, B. A., and Connelly, P. A. (1996) *J. Biol. Chem.* **271,** 695–701
40. Kara, B., Daglioglu, K., Doran, F., Akkiz, H., Sandikci, M., and Kara, I. O. (2009) *Transplant Proc.* **41,** 4401–4404
41. O'Neill, A. J., Cotter, T. G., Russell, J. M., and Gaffney, E. F. (1997) *J. Pathol.* **183,** 325–329
42. Bonny, C., Oberson, A., Negri, S., Sauser, C., and Schorderet, D. F. (2001) *Diabetes* **50,** 77–82
43. Bennett, B. L., Sasaki, D. T., Murray, B. W., O'Leary, E. C., Sakata, S. T., Xu, W., Leisten, J. C., Motiwala, A., Pierce, S, Satoh, Y., Bhagwat, S. S., Manning, A. M., and Anderson, D. W. (2001) *Proc. Natl. Acad. Sci. U.S.A.* **98,** 13681–13686
44. de Waart, D. R., Häusler, S., Vlaming, M. L., Kunne, C., Hänggi, E., Gruss, H. J., Oude Elferink, R. P., and Stieger, B. (2010) *J. Pharmacol. Exp. Ther.* **334,** 78–86

45. Pérez, L. M., Milkiewicz, P., Elias, E., Coleman, R., Sánchez Pozzi, E. J., and Roma, M. G. (2006) *Toxicol. Sci.* **91,** 150–158
46. Kapus, A., Szászi, K., Sun, J., Rizoli, S., and Rotstein, O. D. (1999) *J. Biol. Chem.* **274,** 8093–8102
47. Huang, C., Ni, Y., Wang, T., Gao, Y., Haudenschild, C. C., and Zhan, X. (1997) *J. Biol. Chem.* **272,** 13911–13915
48. Dombrowski, F., Kubitz, R., Chittattu, A., Wettstein, M., Saha, N., and Häussinger, D. (2000) *Biochem. J.* **348,** 183–188
49. Häussinger, D., Kurz, A. K., Wettstein, M., Graf, D., Vom Dahl, S., and Schliess, F. (2003) *Gastroenterology* **124,** 1476–1487
50. Becker, S., Reinehr, R., Graf, D., vom Dahl, S., and Häussinger, D. (2007) *Cell Physiol. Biochem.* **19,** 89–98
51. Klein, N. P., and Schneider, R. J. (1997) *Mol. Cell. Biol.* **17,** 6427–6436
52. Tsygankova, O. M., Peng, M., Maloney, J. A., Hopkins, N., and Williamson, J. R. (1998) *J. Cell Biochem.* **69,** 63–71
53. Mühlfeld, A., Kubitz, R., Dransfeld, O., Häussinger, D., and Wettstein, M. (2003) *Arch. Biochem. Biophys.* **413,** 32–40
54. Schmitt, M., Kubitz, R., Wettstein, M., vom Dahl, S., and Häussinger, D. (2000) *Biol. Chem.* **381,** 487–495
55. Donner, M. G., Schumacher, S., Warskulat, U., Heinemann, J., and Häussinger, D. (2007) *Am. J. Physiol. Gastrointest. Liver Physiol.* **293,** G1134–G1146
56. Crocenzi, F. A., Mottino, A. D., Cao, J., Veggi, L. M., Pozzi, E. J., Vore, M., Coleman, R., and Roma, M. G. (2003) *Am. J. Physiol. Gastrointest. Liver Physiol.* **285,** G449–G459
57. Bastie, C. C., Zong, H., Xu, J., Busa, B., Judex, S., Kurland, I. J., and Pessin, J. E. (2007) *Cell Metab.* **5,** 371–381
58. Fukunishi, S., Tsuda, Y., Takeshita, A., Fukui, H., Miyaji, K., Fukuda, A., and Higuchi, K. (2011) *J. Clin. Biochem. Nutr.* **49,** 20–24
59. Pols, T. W., Noriega, L. G., Nomura, M., Auwerx, J., and Schoonjans, K. (2011) *J. Hepatol.* **54,** 1263–1272
60. Webster, C. R., Blanch, C. J., Phillips, J., and Anwer, M. S. (2000) *J. Biol. Chem.* **275,** 29754–29760
61. Stross, C., Helmer, A., Weissenberger, K., Görg, B., Keitel, V., Häussinger, D., and Kubitz, R. (2010) *Am. J. Physiol. Gastrointest. Liver Physiol.* **299,** G320–G328